Acta Pharmaceutica Sinica B 2025;15(2):707−721

Chinese Pharmaceutical Association
Institute of Materia Medica, Chinese Academy of Medical Sciences

Acta Pharmaceutica Sinica B

www.elsevier.com/locate/apsb
www.sciencedirect.com

ORIGINAL ARTICLE

Safety, dosimetry, and efficacy of an optimized long-acting somatostatin analog for peptide receptor radionuclide therapy in metastatic neuroendocrine tumors: From preclinical testing to first-in-human study

Wei Guo [a,b,†], Xuejun Wen [c,†], Yuhang Chen [b,†], Tianzhi Zhao [d,e,f], Jia Liu [c], Yucen Tao [d,e,f], Hao Fu [a], Hongjian Wang [b], Weizhi Xu [a], Yizhen Pang [a], Liang Zhao [a], Jingxiong Huang [a], Pengfei Xu [d,e,f], Zhide Guo [c], Weibing Miao [g,h,i,*], Jingjing Zhang [d,e,f,*], Xiaoyuan Chen [d,e,f,*], Haojun Chen [a,b,*]

[a]*Department of Nuclear Medicine and Minnan PET Center, Xiamen Key Laboratory of Radiopharmaceuticals, the First Affiliated Hospital of Xiamen University, School of Medicine, Xiamen University, Xiamen 361102, China*
[b]*School of Clinical Medicine, Fujian Medical University, Fuzhou 350005, China*
[c]*State Key Laboratory of Molecular Vaccinology and Molecular Diagnostics & Center for Molecular Imaging and Translational Medicine, School of Public Health, Xiamen University, Xiamen 361102, China*
[d]*Departments of Diagnostic Radiology, Surgery, Chemical and Biomolecular Engineering, and Biomedical Engineering, Yong Loo Lin School of Medicine and College of Design and Engineering, National University of Singapore, Singapore 138667, Singapore*
[e]*Clinical Imaging Research Centre, Centre for Translational Medicine, Yong Loo Lin School of Medicine, National University of Singapore, Singapore 138667, Singapore*
[f]*Nanomedicine Translational Research Program, NUS Center for Nanomedicine, Yong Loo Lin School of Medicine, National University of Singapore, Singapore 138667, Singapore*
[g]*Department of Nuclear Medicine, the First Affiliated Hospital, Fujian Medical University, Fuzhou 350005, China*
[h]*Department of Nuclear Medicine, National Regional Medical Center, Binhai Campus of the First Affiliated Hospital, Fujian Medical University, Fuzhou 350212, China*

*Corresponding authors.
E-mail addresses: miaoweibing@126.com (Weibing Miao), j.zhang@nus.edu.sg (Jingjing Zhang), chen.shawn@nus.edu.sg (Xiaoyuan Chen), leochen0821@foxmail.com (Haojun Chen).
[†]These authors made equal contributions to this work.
Peer review under the responsibility of Chinese Pharmaceutical Association and Institute of Materia Medica, Chinese Academy of Medical Sciences.

https://doi.org/10.1016/j.apsb.2024.05.022

[i]*Fujian Key Laboratory of Precision Medicine for Cancer, the First Affiliated Hospital, Fujian Medical University, Fuzhou 350005, China*

Received 28 February 2024; received in revised form 17 April 2024; accepted 9 May 2024

KEY WORDS

Radiolabeled somatostatin analog;
Neuroendocrine tumor;
Evans blue;
^{177}Lu-LNC1010;
Peptide receptor radionuclide therapy;
First-in-human dose escalation study

Abstract Peptide receptor radionuclide therapy (PRRT) with radiolabeled SSTR2 agonists is a treatment option that is highly effective in controlling metastatic and progressive neuroendocrine tumors (NETs). Previous studies have shown that an SSTR2 agonist combined with albumin binding moiety Evans blue (denoted as ^{177}Lu-EB-TATE) is characterized by a higher tumor uptake and residence time in preclinical models and in patients with metastatic NETs. This study aimed to enhance the *in vivo* stability, pharmacokinetics, and pharmacodynamics of ^{177}Lu-EB-TATE by replacing the maleimide-thiol group with a polyethylene glycol chain, resulting in a novel EB conjugated SSTR2-targeting radiopharmaceutical, ^{177}Lu-LNC1010, for PRRT. In preclinical studies, ^{177}Lu-LNC1010 exhibited good stability and SSTR2-binding affinity in AR42J tumor cells and enhanced uptake and prolonged retention in AR42J tumor xenografts. Thereafter, we presented the first-in-human dose escalation study of ^{177}Lu-LNC1010 in patients with advanced/metastatic NETs. ^{177}Lu-LNC1010 was well-tolerated by all patients, with minor adverse effects, and exhibited significant uptake and prolonged retention in tumor lesions, with higher tumor radiation doses than those of ^{177}Lu-EB-TATE. Preliminary PRRT efficacy results showed an 83% disease control rate and a 42% overall response rate after two ^{177}Lu-LNC1010 treatment cycles. These encouraging findings warrant further investigations through multicenter, prospective, and randomized controlled trials.

1. Introduction

Neuroendocrine tumors (NETs) frequently demonstrate elevated levels of somatostatin receptor (SSTR) expression, with a predominance of subtype 2 (SSTR2), allowing for imaging and peptide receptor radionuclide therapy (PRRT) utilizing diolabeled somatostatin analogs (SSAs)[1−4]. Recently, the efficacy and safety of the peptide-based radiopharmaceutical, ^{177}Lu-DOTATATE (Lutathera), were demonstrated in the randomized controlled trial NETTER-1 involving patients with well-differentiated metastatic or locally advanced midgut NETs, leading to regulatory approval by the European Medicines Agency and US Food and Drug Administration[3].

A possible downside of ^{177}Lu-DOTATATE is its swift blood clearance, resulting in relatively short tumor retention. Evans blue (EB) is a promising albumin-binding component with a strong affinity for serum albumin binding site 1, enabling prolonged circulation of targeting molecules conjugated with EB derivatives[5,6]. The SSTR2 agonist, DOTATATE, has been conjugated with truncated EB (EB-TATE) and radiolabeled with ^{177}Lu for use as a long-lasting radiolabeled SSA (^{177}Lu-EB-TATE) for PRRT. Preclinical studies have shown that ^{177}Lu-EB-TATE exhibits a 4-fold higher tumor-absorbed dose and greater anti-tumor efficacy than that of ^{177}Lu-DOTATATE[6,7]. Preliminary clinical studies also indicated a 7.9-fold higher tumor-absorbed dose than that of ^{177}Lu-DOTATATE[8]. Notably, patients in the high-dose group (3.7 GBq/cycle) tended to demonstrate a reduced disease control rate (DCR) after multiple treatment cycles than those in the median-dose group (2.2 GBq/cycle)[9]. When devising radiation therapy plans, dose escalation is deemed as a passive strategy to enhance tumor treatment effectiveness. However, optimizing drug pharmacokinetics is fundamental for reducing the frequency of injections, increasing the absorbed dose in target lesions, and enhancing the overall effectiveness of drug therapy.

Maleimides, as intermediates between EB and SSAs, are combined with reactive thiol compound groups using Michael-type addition owing to their unique selectivity, mild reaction conditions, and rapid reaction kinetics[10]. However, maleimides often form unstable thiosuccinimide bonds in physiological settings, particularly in the presence of compounds with thiol groups. This instability is potentially due to elimination reactions that occur through thiol-disulfide exchange with endogenous thiols, such as glutathione (GSH) and albumin[11], which can lead to suboptimal pharmacodynamic, pharmacokinetic, and safety characteristics.

Evidence suggests a payload release rate from structures containing thiosuccinimide in plasma that varies between 50% and 75% over a period of 7−14 days[10]. As carcinoma cells exhibit elevated GSH levels, exceeding those of normal cells over 1000 times[12], the high sensitivity of maleimide-thiol groups to GSH and albumin thiols may potentially affect ^{177}Lu-EB-TATE uptake and retention in tumors. Therefore, the unresolved drawbacks of ^{177}Lu-EB-TATE remain a barrier to optimization.

Conjugation with polyethylene glycol (PEG) is a commonly employed method to enhance the pharmacokinetic properties of targeting molecules. In recent studies, several Evans blue derivatized compounds (*e.g.*, EB-PSMA and EB-FAPI) were successfully modified by replacing the maleimide-thiol linker with a polyethylene glycol (PEG) chain. This modification strategy led to the development of radiopharmaceuticals that demonstrated

significantly improved tumor uptake and retention in preclinical studies[13,14].

In this study, we developed an optimized EB-modified SSA, LNC1010, which conjugated the PEG chain through the thiol group as an alternative intermediate to maleimide for improved pharmacokinetics and pharmacodynamics. Following preclinical *in vitro* and *in vivo* biological evaluation, we conducted a first-in-human, dose-escalation study to investigate the safety, tolerability, pharmacokinetics, dosimetry, and preliminary efficacy of ^{177}Lu-LNC1010 in patients with advanced/metastatic SSTR2-positive NETs. Moreover, we compared our findings with those of ^{177}Lu-EB-TATE-based PRRT.

2. Materials and methods

2.1. Patients

This single-center, open-label, non-randomized, first-in-human, and dose-escalation investigator-initiated trial was conducted at the First Affiliated Hospital of Xiamen University in Xiamen, China. This study received Institutional Review Board approval and complied with the tenets of the Declaration of Helsinki. This study was registered at ClinicalTrials.gov (registration number: NCT05410743). The use of ^{177}Lu-LNC1010 was approved by the hospital's multidisciplinary tumor board. All enrolled patients provided written informed consent.

We included patients aged >18 years with histologically confirmed NETs, unresectable measurable disease, progressive metastatic disease after SSA and/or post-tyrosine kinase inhibitor treatment (according to RECIST version 1.119), and who had no fewer than one lesion demonstrating greater uptake than that of normal liver tissue at baseline ^{68}Ga-DOTATATE PET/CT. The criteria for exclusion were a platelet count below 50×10^9/L, a white-cell count less than 2.0×10^9/L, a total bilirubin level more than 3 times the upper limit of the normal range, a serum albumin level below 2.0 g/dL, a hemoglobin level less than 8.0 g/dL, a serum creatinine level exceeding 150 μmol/L, cardiac insufficiency including carcinoid heart valve disease, severe allergy or hypersensitivity to radiographic contrast material, claustrophobia, and pregnancy or lactation.

2.2. Animal model establishment

All mice experiments were approved by the relevant Animal Care and Use Committee, and performed in compliance with animal experimentation related national laws. The right upper limbs of 6-week-old male BALB/c nude mice were subcutaneously injected with AR42J tumor cells (5×10^6). When the tumor volume reached about 200−300 mm^3, micro-PET imaging, micro-single-photon emission computerized tomography SPECT imaging, and biodistribution studies were performed.

2.3. ^{177}Lu-LNC1010 synthesis and radiolabeling

The detailed synthesis process, purification methods, and chemical characterizations of LNC1010 are shown in the Supporting Information For ^{177}Lu-LNC1010 radiolabeling, 370−740 MBq $^{177}LuCl_3$ was mixed with LNC1010 (100−200 μg) and diluted with 0.2 mL of 0.5 mol/L NaOAc (pH = 5.5) and heated reaction at 95 °C for 30 min. The specific activity of ^{177}Lu-LNC1010 is about 18.5−37 MBq/nmol. ^{177}Lu-DOTATATE and ^{177}Lu-EB-TATE were radiolabeled using the same method. *In vivo* metabolism studies were performed using ^{68}Ga-LNC1010 and ^{68}Ga-EB-TATE injections, which with the similar specific activities of 18.5−37 MBq/nmol. After 2 h of the injection, urine samples were collected for the detection of radio-high-performance liquid chromatography (HPLC).

2.4. In vitro cell uptake and receptor-binding assays

SSTR2-expressing rat amphicrine pancreatic AR42J cells were obtained from the American Type Culture Collection and incubated in F12K medium, which containing 20% fetal bovine serum (FBS), at 37 °C in 5% CO_2. For cellular uptake assays, AR42J cells were seeded in a 24-well plate at approximately 2×10^5/well and subsequently incubated with 0.5 mL 37 kBq of ^{177}Lu-LNC1010 (specific activity is 18.5 MBq/nmol) in F12K medium for 10, 30 min, 2, 4, and 24 h at 37 °C. For the blocking assay, unlabeled LNC1010 (50 μg/mL) was added into the cells as an inhibitor to identify the targeted specificity. For SSTR2 receptor-binding assays, 4×10^5 AR42J cells were incubated with varying unlabeled LNC1010 or DOTATATE concentrations (10^{-5}−10^{-12} mol/L) with 7.4 kBq ^{177}Lu-DOTATATE (specific activity is 18.5 MBq/nmol) for 1 h at 37 °C, and the supernatant was removed at the specific time points. Then, the cells were washed twice with ice-cold phosphate-buffered saline (PBS) and finally lysed with NaOH (1 mol/L). The radioactivity of cell lysates was determined with a γ-counter (Wizard 2480; PerkinElmer Inc., USA). Each experiment was repeated three times. Binding affinity was calculated using GraphPad Prism software (USA) by nonlinear regression.

2.5. Validation of the docking method

Before conducting the docking study, preliminary docking calculations were executed utilizing the original substrates found in the crystal structures (PDB ID: 7XNA and 2BXC) to assess the efficacy of the docking and scoring methodologies. The substrates, namely TATE and phenylbutazone, were subjected to docking simulations within the binding sites of somatostatin receptor (SSTR) and human serum albumin (HSA) employing GLIDE. Subsequent to these simulations, PymoL was employed to align the docked poses with their respective initial poses for both compounds, resulting in calculated Root Mean Square Deviation (RMSD) values of 1.036 and 1.517 for TATE and phenylbutazone, respectively. This analysis collectively underscores the versatility of our docking methods, thereby affirming their applicability as robust models in further docking study.

2.6. In vivo evaluation of ^{68}Ga-LNC1010 and ^{177}Lu-LNC1010

For micro-PET imaging, approximately 7.4 MBq ^{68}Ga-LNC1010, ^{68}Ga-EB-TATE, or ^{68}Ga-DOTATATE (specific activities of these three radiotracers are 37 MBq/nmol) was injected into the AR42J tumor model for 10-min static PET imaging, about 0.2 nmol precursors mass were injected into mice. At 0.5, 2, and 4 h, the mice were anesthetized with 2% isoflurane and placed on a micro-PET/CT scanner (Inveon; Siemens Medical Solutions, USA) for imaging acquisition. Blocking assays were performed by injecting 50-fold excess unlabeled LNC1010 while administering ^{68}Ga-DOTATATE. For SPECT/CT imaging, approximately 18.5 MBq of ^{177}Lu-LNC1010 (37 MBq/nmol) or ^{177}Lu-EB-TATE (37 MBq/nmol) was injected intravenously into the AR42J tumor mice, about 0.5 nmol precursors mass were injected into mice.

Whole-body SPECT/CT images were acquired using the nano-Scan scanner (Mediso Ltd., Hungary) at 1, 4, 24, 48, 72, and 96 h post-injection. The acquisition parameters of SPECT/CT were as follows: energy peaks for ^{177}Lu are 56.1, 112.9, and 208.4 keV; window width is 20%; matrix is 256 × 256; frames are 48. The duration of SPECT image acquisition was about 30 min, and the same mouse was utilized for all time points. For the biodistribution study, AR42J tumor mice were intravenously injected with 1.48 MBq (specific activities are 18.5 MBq/nmol) of ^{177}Lu-LNC1010, ^{177}Lu-EB-TATE, or ^{177}Lu-DOTATATE, respectively, about 0.08 nmol precursors mass were injected into mice. The mice were then sacrificed at different time points (n = 3/group), the interested organs and tumor tissues were collected and weighed. Radioactivities of these tissues were detected using the γ-counter (Wizard 2480; PerkinElmer Inc., USA), and the biodistribution results were quantitatively represented with the percentage of injected dose per gram (%ID/g).

2.7. ^{177}Lu-LNC1010 clinical trials in NETs

The study employed a classic 3 + 3 dose-escalation design with an 8-week interval. Patients were randomly assigned to the different dosage groups based on the order of enrollment. Based on previous EB-derivative study[15], the starting dose of ^{177}Lu-LNC1010 investigated was 2.22 GBq (60 mCi). Subsequent groups received a dose that was increased by 50% increments until dose-limiting toxicity (DLT) was observed. Initially, the first dosage group consisted of three patients (2.22 GBq per cycle). If none of the patients in a group experienced DLT, an additional trio of patients would be enrolled to receive the next elevated dosage level. Should one out of the three patients at any given dosage level experience DLT, a further three patients were recruited to receive the same dosage level. The peak dosage, where no more than one patient out of six exhibited DLT, was deemed the maximum tolerated dosage. DLT was defined as any ^{177}Lu-LNC1010-related adverse event (AE) ≥G3 in accordance with the National Cancer Institute Common Terminology Criteria for Adverse Events, version 5.0. For comparison, PRRT with ^{177}Lu-EB-TATE was performed in three patients with a fixed dose (3.33 GBq of ^{177}Lu-EB-TATE) according to previous research [16].

2.8. Scintigraphy and SPECT/CT imaging

No special preparatory measures were needed on the day of ^{177}Lu-LNC1010 administration. The ^{177}Lu-LNC1010 was diluted with 100 mL of 0.9% saline and slowly administered intravenously over a period of 20−30 min. Patients were closely monitored for any symptoms and vital signs throughout the process. The treatment regimen was designed for two cycles, with an eight-week interval between cycles.

^{177}Lu-LNC1010 kinetics were determined based on planar scintigraphic whole-body scans (WBS) (anterior/posterior) at 1, 4 h, 1, 2, 3, 4, and 7 day after radiopharmaceutical administration. An additional whole-body SPECT/CT scan was performed on each patient on Day 3 following administration. Image acquisition was conducted using a double-head γ-camera (Symbia T16; Siemens Medical Solutions, Malvern, PA, USA) equipped with a low-energy, high-resolution parallel-hole collimator at the First Affiliated Hospital of Xiamen University. The settings for the acquisition parameters were as follows: an energy window of 15% centered on a peak value of 208 keV; the scanning speed for whole-body imaging was set to 10 cm/min, with each frame having an exposure time of 20 s, resulting in a total of 32 frames. Specific scanning parameters are described in the Supporting Information.

2.9. Dosimetry calculation

The dosimetry for each patient was estimated in the first treatment cycle using a previously published procedure[17−19]. The patients were instructed to hold their urine before the initial scan. Therefore, the total-body counts measured during the first whole-body scan were defined as 100% of the administered activity. Regions of interest were manually delineated on the acquired scintigraphic images by a physicist in collaboration with a nuclear medicine physician, selecting lesions with the highest uptake suitable for dosimetry. Analysis was performed using the Hermes system (Hermes Medical Solutions, Stockholm, Sweden). SPECT/CT scans were reconstructed and quantified using Hermes standardized uptake value (SUV) SPECT software, and mean absorbed doses in organs and tumors were estimated with the built-in OLINDA/EXM 2.1 software. The dosimetry protocol was used to evaluate parameters such as uptake as a fraction of the administered activity (%AA), mean absorbed dose in unaffected organs (mSv/MBq), tumor-absorbed dose (Gy/GBq), effective half-life (h), and residence time (h).

2.10. Safety

During and after the treatment, patients were hospitalized for at least 3−5 days to monitor and record potential side effects such as pain, nausea, vomiting, and dyspnea. Structured questionnaires were employed to detect any complications that emerged later on. Hematologic, renal, and liver function tests were performed before administration of ^{177}Lu-LNC1010 and every 2 weeks thereafter. All treatment-related AEs were documented in accordance with the National Cancer Institute's Common Terminology Criteria for Adverse Events, version 5.0.

2.11. Response assessment

The anti-tumor response to ^{177}Lu-LNC1010 was monitored every 8 weeks following each treatment cycle using functional imaging modalities, which included ^{68}Ga-DOTATATE PET/CT and contrast-enhanced CT/MR. Tumor responses were categorized according to RECIST 1.1 criteria, and the overall response rate (ORR) as well as the disease control rate (DCR) were evaluated.

2.12. Statistics analyses

Data statistical analyses were performed using SPSS (IBM SPSS Statistics for Windows, version 21.0; Armonk, NY, USA) and GraphPad Prism software. Quantitative data are presented as mean ± standard deviation (SD). The mean values were compared using a Mann−Whitney U test. Data that were not normally distributed are reported as the median along with the interquartile range. Statistical significance was determined at $P < 0.05$.

3. Results

3.1. LNC1010 synthesis and radiolabeling

The chemical structures of ^{177}Lu/^{68}Ga-LNC1010 and ^{177}Lu/^{68}Ga-EB-TATE are shown in Fig. 1. The synthesis route of LNC1010 is

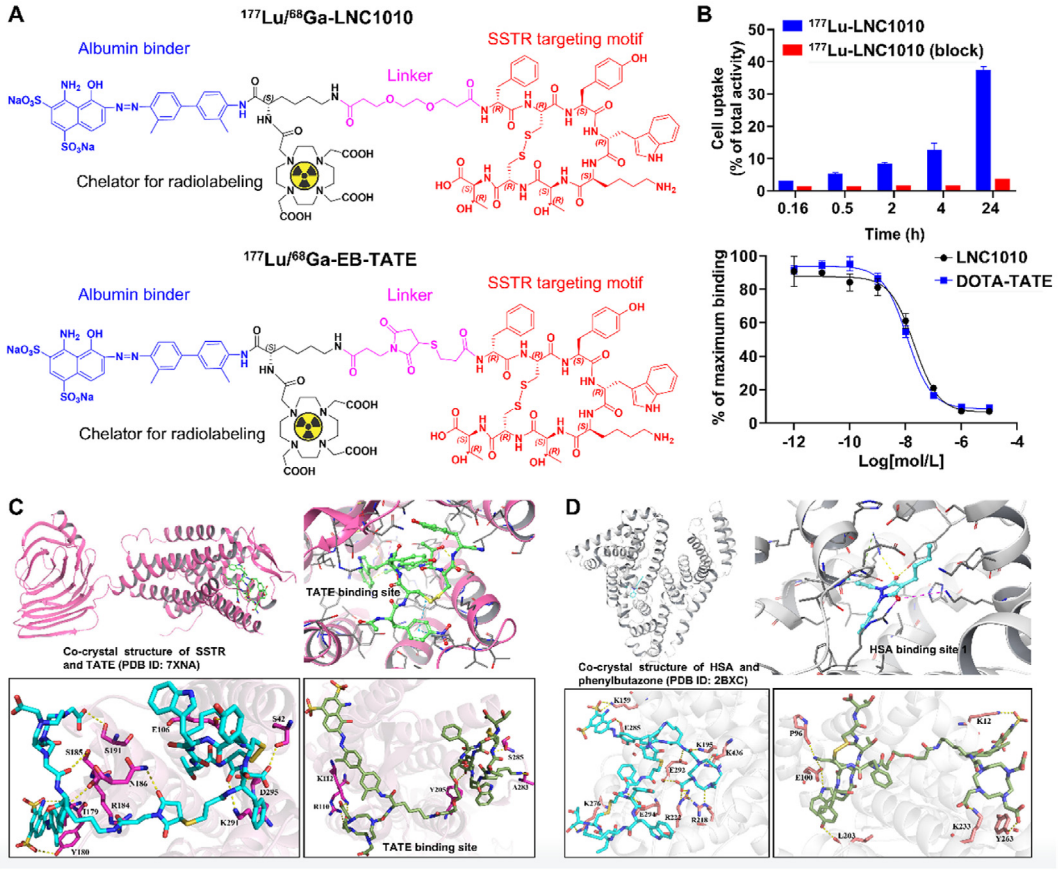

Figure 1 (A) Chemical structures of ^{177}Lu/^{68}Ga-LNC1010 and ^{177}Lu/^{68}Ga-EB-TATE. (B) Cellular uptake assay with ^{177}Lu-LNC1010 and blocking experiment with unlabeled LNC1010 in AR42J tumor cells; competition-binding assays with LNC1010 (IC_{50} = 20.65 ± 6.02 nmol/L) and DOTATATE (IC_{50} = 11.49 ± 1.58 nmol/L). (C) Predicted binding mode of EB-TATE and LNC1010 with SSTR (PDB ID: 7XNA. Yellow dashed lines indicated in this figure are hydrogen bonds). (D) Predicted binding mode of EB-TATE and LNC1010 with HSA (PDB ID: 2BXC).

shown in Supporting Information Fig. S1. LNC1010 and its intermediate products underwent characterization using mass spectrometry and HPLC (Supporting Information Figs. S2−S6). As shown in Supporting Information Fig. S7A, ^{68}Ga-LNC1010 remained mostly stable (>99%) after 2-h incubation in saline, GSH solution, and urine. Conversely, the radiochemical purity of ^{68}Ga-EB-TATE significantly decreased, with several new peaks emerging after 2-h incubation in GSH solution and urine (Fig. S7B), indicating ^{68}Ga-EB-TATE instability in GSH solution and *in vivo*.

3.2. *Cellular uptake and binding affinity assays*

AR42J cell uptake of ^{177}Lu-LNC1010 gradually increased over time, peaking at 24 h (36.96 ± 1.60%). Significant radioligand uptake inhibition was observed following 50 μg/mL unlabeled LNC1010 application (3.37 ± 0.17%; 90.88% reduction), confirming specific binding to SSTR2 (Fig. 1B). The ligand concentration required for 50% inhibition (IC_{50}) values of LNC1010 and DOTATATE were similar (20.65 ± 6.02 *vs.* 11.49 ± 1.58 nmol/L), suggesting comparable receptor-binding affinity for SSTR2 (Fig. 1C) and negligible EB modification strategy-related effects on SSTR2 binding affinity.

3.3. *Docking study*

Molecular docking was applied to predict the potential binding mode of EB-TATE and LNC1010. As shown in Fig. 1C, predicted conformations of EB-TATE (docking score: −9.463) and LNC1010 (docking score: −8.759) were well docked into the binding site of SSTR, and formulated numerous hydrogen bonds with surrounding residues which demonstrated the reasonableness of our radioligand design. Next, we have simulated the potential binding modes of two compounds with albumin. Since Evans blue (EB) was reported to binding in the HSA binding site 1, we have chosen site 1 as the potential binding site to carry out the docking study. As a result, EB-TATE and LNC1010 exhibited favorable binding poses, with docking scores of −9.103 and −7.093 respectively (Fig. 1D).

3.4. *In vivo evaluation of ^{68}Ga-LNC1010 and ^{177}Lu-LNC1010*

Representative static microPET images of AR42J tumor xenografts are shown in Fig. 2A−C. ^{68}Ga-LNC1010 tumor uptake was significantly higher than that of ^{68}Ga-EB-TATE at 2 h (16.08 ± 1.26 *vs.* 8.67 ± 1.46% ID/g, P = 0.003) and 4 h post injection (22.42 ± 1.28 *vs.* 12.25 ± 1.52 %ID/g, P < 0.001) (Fig. 2A and B), while ^{68}Ga-DOTATATE tumor uptake was 7.33 ± 1.91 and 6.67 ± 1.94% ID/g at 2 and 4 h post injection, respectively (Fig. 2C). The tumor to muscle (9.81 ± 0.32) and tumor to kidney ratios (2.02 ± 0.23) of ^{68}Ga-LNC1010 were higher than ^{68}Ga-EB-TATE (5.39 ± 0.97 and 1.16 ± 0.19, respectively) at 4 h post injection. The blocking assay demonstrated significant inhibition of tumor uptake by unlabeled

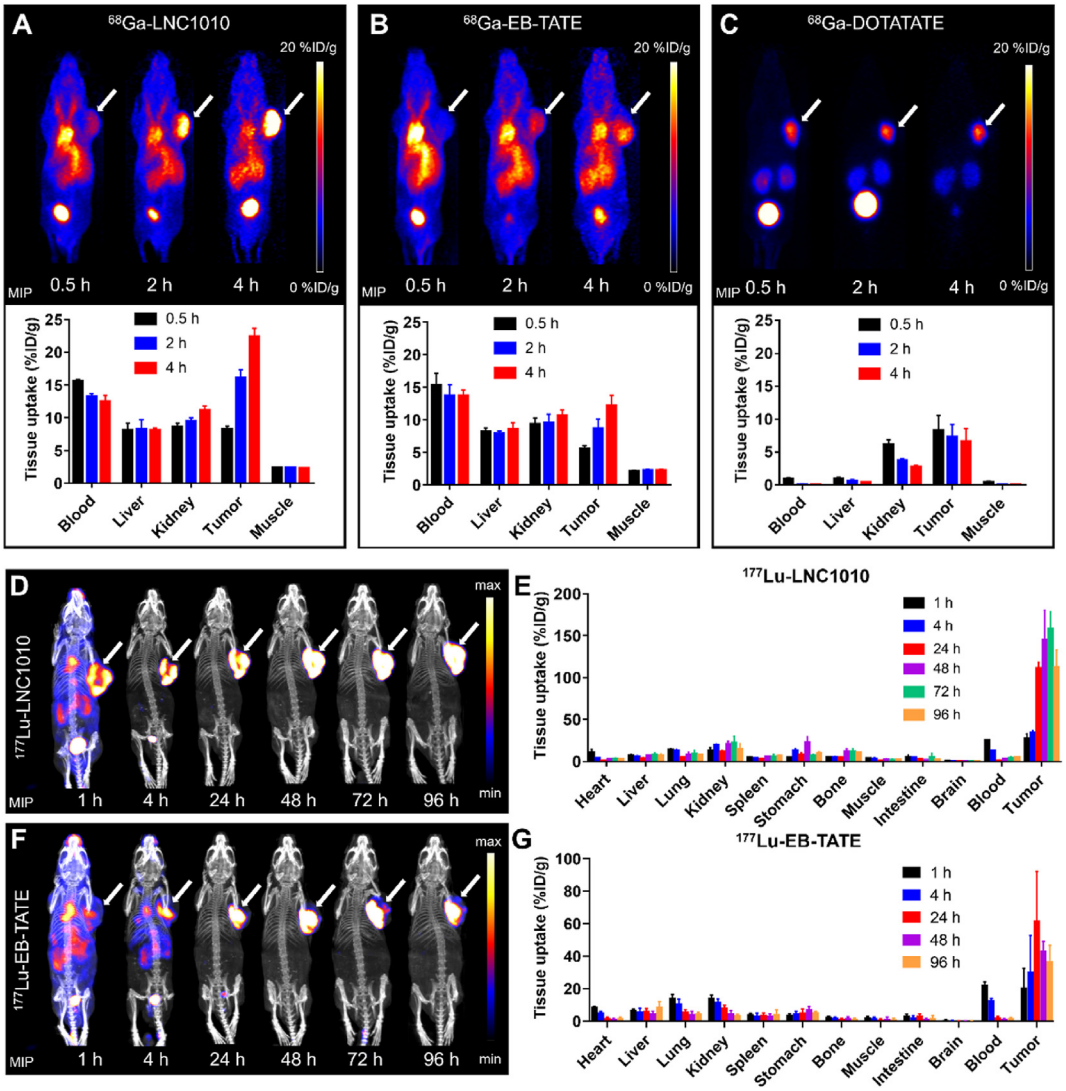

Figure 2 Micro-PET imaging and quantitative tissue uptake of ^{68}Ga-LNC1010 (A), ^{68}Ga-EB-TATE (B) and ^{68}Ga-DOTATATE (C) in AR42J tumor-bearing mice at 0.5, 2, and 4 h post injection (three mice/group). SPECT/CT images of ^{177}Lu-LNC1010 (D) and ^{177}Lu-EB-TATE (F) in AR42J tumor-bearing mice at 1, 4, 24, 48, 72, and 96 h post injection (three mice/group). *Ex vivo* biodistribution of ^{177}Lu-LNC1010 (E) and ^{177}Lu-EB-TATE (G) in AR42J tumor-bearing mice at different time points. MIP: maximum-intensity-projection.

LNC1010 in the AR42J tumor-bearing mice (Supporting Information Fig. S8A and S8B). ^{68}Ga-DOTATATE tumor uptake decreased from 7.33 ± 1.91 to 0.37 ± 0.17%ID/g (approximately 95%) at 2 h post injection after blocking with 50-fold excess LNC1010 (Fig. S8C and S8D).

Representative SPECT/CT images of the AR42J tumor mice are shown in Fig. 2D−F. Substantial ^{177}Lu-LNC1010 tumor uptake was observed at 1 h post injection. Blood uptake of ^{177}Lu-LNC1010 gradually decreased to baseline levels at 24 h post tracer injection, whereas tumor uptake increased in a time-dependent manner and remained high until 96 h post injection. ^{177}Lu-LNC1010 uptake in the kidneys gradually decreased and was significantly lower than that in the tumor at all time points (Supporting Information Fig. S9A). High tumor-to-blood (45.78 ± 6.44), tumor-to-liver (25.92 ± 9.38), tumor-to-kidney (18.76 ± 2.13), and tumor-to-muscle (129.66 ± 16.82) uptake ratios were observed at 96 h post-injection (Fig. S9C). SPECT/CT images exhibited lower ^{177}Lu-EB-TATE tumor uptake (77.86 ± 5.04 *vs.* 159.67 ± 40.11, $P = 0.02$) at 96 h post-injection than that of ^{177}Lu-LNC1010 (Fig. 2D and F; Fig. S9A and S9B). ^{177}Lu-EB-TATE exhibited lower tumor-to-blood (17.93 ± 2.00), tumor-to-liver (7.53 ± 1.24), tumor-to-kidney (8.88 ± 0.95), and tumor-to-muscle (45.08 ± 5.23) uptake ratios at 96 h post injection than those of ^{177}Lu-LNC1010 (Fig. S9C and S9D).

3.5. *Biodistribution study*

Tumor uptake of ^{177}Lu-LNC1010 gradually increased and peaked at 72 h post injection (126.44 ± 16.01 %ID/g), maintaining a high level even at 96 h post injection (95.28 ± 17.43 %ID/g). Tumor uptake was considerably greater than uptake in the unaffected organs, including the kidneys (12.84 ± 5.25 %ID/g), spleen (5.56 ± 1.14 %ID/g), and liver (6.30 ± 1.36 %ID/g) (Fig. 2E). In contrast, ^{177}Lu-EB-TATE tumor uptake was lower than that of ^{177}Lu-LNC1010 (37.28 ± 9.50 *vs.* 95.28 ± 17.43 %ID/g,

$P = 0.005$) at 96 h post-injection (Fig. 2E–G). ^{177}Lu-DOTATATE tumor uptake was relatively low (9.19 ± 2.16 %ID/g) at 48 h post-injection, with the highest tumor uptake of 15.49 ± 6.48 %ID/g at 4 h post injection (Supporting Information Fig. S10). Overall, these preclinical results suggested that ^{177}Lu-LNC1010 may be superior to ^{177}Lu-DOTATATE and ^{177}Lu-EB-TATE for PRRT in SSTR2-positive NETs, due to its high tumor uptake and high stability *in vivo*.

3.6. *Patients*

In total, 12 patients with metastatic NETs (median age, 55 years; range, 37–66 years) were enrolled in this study. The patients' characteristics are summarized in Table 1. Patients underwent two ^{177}Lu-LNC1010 PRRT cycles, with three patients receiving 2.22 GBq/cycle (Group A), six receiving 3.33 GBq/cycle (Group B), and three receiving 4.99 GBq/cycle (Group C). Three other patients were treated with ^{177}Lu-EB-TATE at a fixed dose of 3.33 GBq/cycle (Group D) for comparison. The most frequent primary site of the tumor was the pancreas (40%, 6/15). All patients had metastatic tumors, most commonly in the lymph nodes (80%, 12/15), bone (67%, 10/15), and liver (60%, 9/15). Eight (53%) were categorized as intermediate (Grade 2), six (40%) as low (Grade 1), and one (7%) as high (Grade 3) NETs, respectively. The flowchart of the study design is shown in Fig. 3.

3.7. *Safety and toxicity*

The hematologic toxicity grades are outlined in Table 2. Subacute hematologic toxicity related to ^{177}Lu-LNC1010 was observed in 83% patients (10/12) during the observation period, with the majority of AEs being G1 or G2 (7/12, 58%). G3/G4 hematologic toxicity was observed in three patients (3/12, 25%). In Group A, Patient 2 experienced G2 granulocytopenia following the second PRRT cycle, while Patient 3 exhibited G1/G2 granulocytopenia, leukopenia, and thrombocytopenia after two treatment cycles. In Group B, Patient 4 experienced G3 leukopenia and G4 thrombocytopenia 4 weeks after the second ^{177}Lu-LNC1010 administration, leading to the enrollment of three additional patients in this group (Patients 7–9), none of whom developed G3/G4 hematologic AEs. In Group C, Patients 10 and 12 experienced G3/G4 hemoglobinemia and G4 thrombocytopenia, preventing further dose escalation. For these two patients, the hematologic toxicity began 4–6 weeks after the second ^{177}Lu-LNC1010 administration and persisted for 6–10 weeks. Non-hematologic AEs related to ^{177}Lu-LNC1010 occurred in 33% of patients (4/12) and consisted of G1 abdominal pain (2/12, 17%), G1 vomiting (1/12, 8%), and G2 asthenia (1/12, 8%). These AEs mostly resolved before the next treatment cycle. Further details are presented in Supporting Information Table S1. Therefore, an identified therapeutic dose of 3.33 GBq/cycle was identified for future clinical trials based on these findings.

To ascertain the correlation between the cumulative red bone marrow dose (RMD) estimated for two therapeutic cycles and the rate of hematological toxicity, G3/G4 thrombocytopenia served as the endpoint for toxicity. Altogether, 75% (3 out of 4) of the patients who were subjected to more than 1.5 Gy of marrow doses experienced G3/G4 thrombocytopenia, leukopenia, and neutropenia subsequent to two cycles of ^{177}Lu-LNC1010 treatment (Table 2), whereas those treated with <1.2 Gy did not develop any G3/G4 AEs.

Table 1 Demographic and baseline clinical characteristics of patients.

Patient	Age (year)	Sex	Primary tumor	Grade	Ki-67	Metastases	Time since diagnosis (year)	Relevant previous surgery	Endocrine treatments	Other relevant treatment	Symptoms before PRRT	Dose (GBq)
LNC1010-1	55	F	Thyroid	G1	3%	LN	12	Radical thyroidectomy	None	TKI	None	2.22
LNC1010-2	44	M	Pancreas	G2	8%	LN, liver	8	Pancreatectomy	SSA	TACE/TAE	None	2.22
LNC1010-3	65	F	Liver	G2	15%	LN, bone	0.5	None	SSA	None	None	2.22
LNC1010-4	62	M	Pancreas	G2	10%	LN, bone, liver	0.75	None	SSA	Denosumab	None	3.33
LNC1010-5	63	M	Pancreas	G1	1.5%	LN, bone, liver	7	Pancreatectomy	SSA	TACE/TAE, chemotherapy, TKI	None	3.33
LNC1010-6	44	M	Rectum	G1	1%	LN, bone, liver	4	None	SSA	TACE/TAE, chemotherapy	Constipation	3.33
LNC1010-7	66	M	Prostate	G3	34%	Bone	5	None	Leuprorelin acetate, ODM-21	Chemotherapy	Bone pain	3.33
LNC1010-8	55	F	Pancreas	G1	<2%	LN, bone, liver	12	Pancreatectomy	SSA	Chemotherapy, TKI	Abdominal pain, vomiting	3.33
LNC1010-9	51	M	Kidney	G2	5%	Bone	5	Left nephrectomy	None	TKI, tislelizumab	Bone pain	3.33
LNC1010-10	58	F	Stomach	G1	1%	LN, liver	1	None	SSA	TACE/TAE, chemotherapy, TKI	Nausea	4.99
LNC1010-11	37	F	Pancreas	G1	2%	Liver, spleen	0.5	None	SSA	None	Hypoglycemia symptoms	4.99
LNC1010-12	51	F	Liver	G2	None	LN, bone	9	None	SSA	TACE/TAE	None	4.99
EB-TATE-1	71	M	Rectum	G2	5%	LN, bone, liver	3	None	SSA	TACE/TAE, chemotherapy, TKI	Abdominal distension	3.33
EB-TATE-2	28	M	Mediastinum	G2	15%	LN, bone	3	Enlarged thymectomy	None	Chemotherapy, enosumab	None	3.33
EB-TATE-3	36	F	Pancreas	G2	None	LN, liver	5	Pancreatectomy	SSA	TKI	None	3.33

LN: lymph node; SSA: somatostatin analog; TACE: trans-arterial chemoembolization; TAE: trans-arterial embolization; TKI: tyrosine kinase inhibitor; ODM-201: Darolutamide.

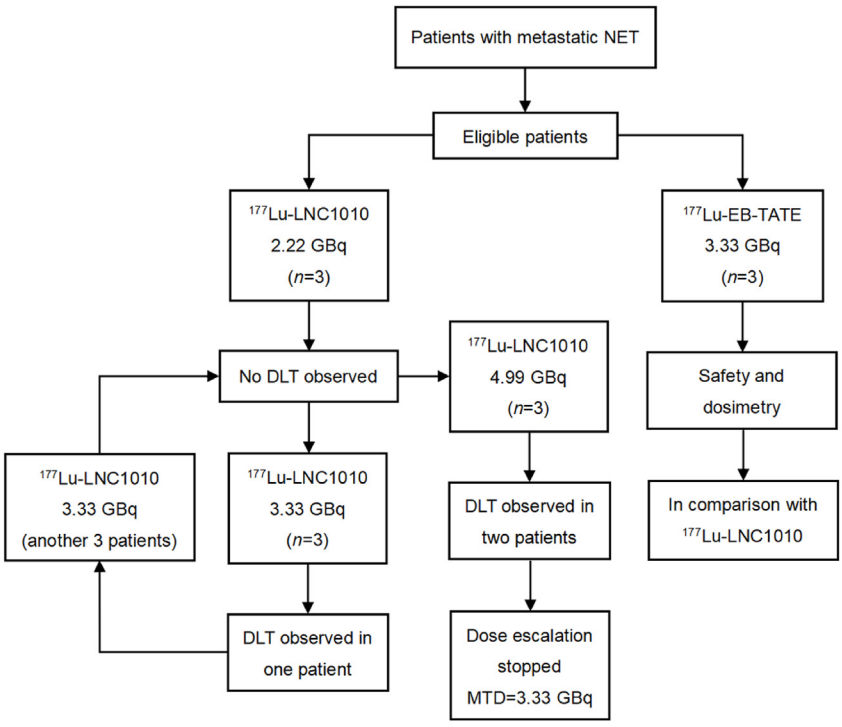

Figure 3 Participant flow chart of the traditional 3 + 3 dose-escalation study design with ^{177}Lu-LNC1010 and a comparison with ^{177}Lu-EB-TATE. DLT: dose-limiting toxicity; MTD: maximum tolerated dose.

In Group D, hematotoxicity was observed in all three patients, including one case with G3 thrombocytopenia 4 weeks after the first PRRT cycle (resolved before the commencement of the second cycle) and G3 granulocytosis and thrombocytopenia 4 weeks after the second cycle. Among the 15 patients who underwent either ^{177}Lu-LNC1010 or ^{177}Lu-EB-TATE PRRT, two patients (LNC1010-12 and EB-TATE-03) experienced an extended gap between the two cycles of 3 and 2 weeks, respectively, owing to delayed recovery from hematologic toxicity (Supporting Information Table S2).

G3 hepatotoxicity was observed in two patients from Groups C and D (Table 2). No patients experienced nephrotoxicity of any grade related to ^{177}Lu-LNC1010 or ^{177}Lu-EB-TATE administration.

3.8. *Pharmacokinetics profile*

Post-therapeutic planar WBS demonstrated relatively high ^{177}Lu-LNC1010 uptake in the blood pool 1 h post injection, and in certain tumor lesions 1 h post-injection, becoming more pronounced 4 h post injection. Serial WBS between 24 and 168 h post injection showed high ^{177}Lu-LNC1010 uptake at all metastasis sites in all patients (Fig. 4), indicating prolonged intra-tumor retention activity. In contrast, ^{177}Lu-LNC1010 uptake in unaffected organs, including the bloodstream, reduced to baseline levels after 24 h, gradually decreasing over time. Similar to ^{177}Lu-LNC1010, intense uptake and prolonged retention of ^{177}Lu-EB-TATE in tumor lesions in the serial WBS was observed. However, ^{177}Lu-EB-TATE uptake in unaffected organs, including the heart, main blood vessels, and muscles, was higher than that of ^{177}Lu-LNC1010, resulting in a lower tumor-to-baseline ratio at the various time points (Supporting Information Fig. S11).

3.9. *Dosimetry evaluation*

Dosimetry was calculated using OLINDA/EXM software based on SPECT image quantification (Table 3). No significant difference in whole-body mean effective dose was observed between ^{177}Lu-LNC1010 and ^{177}Lu-EB-TATE (0.23 ± 0.06 *vs.* 0.23 ± 0.08 mSv/MBq, P = 1.00). The spleen had the highest absorbed dose of 2.53 ± 2.13 mSv/MBq and 2.27 ± 0.04 mSv/MBq for ^{177}Lu-LNC1010 and ^{177}Lu-EB-TATE, respectively (P = 0.93). However, ^{177}Lu-LNC1010 had somewhat lower absorbed dose in the kidneys than that of ^{177}Lu-EB-TATE (1.91 ± 0.60 *vs.* 2.47 ± 0.48 mSv/MBq, P = 0.15), whereas ^{177}Lu-LNC1010 had a higher absorbed dose than that of ^{177}Lu-EB-TATE in the liver (0.25 ± 0.18 *vs.* 0.07 ± 0.00 mSv/MBq, P = 0.30). Both radiopharmaceuticals exhibited similar absorbed radiation doses in the red bone marrow (0.17 ± 0.04 *vs.* 0.15 ± 0.02 mSv/MBq, P = 0.30), pancreas (0.20 ± 0.03 *vs.* 0.20 ± 0.02 mSv/MBq, P = 0.95), and urinary bladder wall (0.32 ± 0.08 *vs.* 0.32 ± 0.10 mSv/MBq, P = 1.00).

The kinetics of ^{177}Lu-LNC1010 and ^{177}Lu-EB-TATE observed following administration are depicted in Fig. 5. Regarding the whole-body kinetics, the time−activity curves for both agents declined at a constant rate. The whole-body effective half-life (105.14 ± 12.26 h *vs.* 111.27 ± 7.58 h, P = 0.57) and residence time (148.71 ± 15.10 h *vs.* 166.97 ± 8.75 h, P = 0.04) of ^{177}Lu-LNC1010 were slightly shorter than those of ^{177}Lu-EB-TATE. However, ^{177}Lu-LNC1010 exhibited higher tumor uptake and a 3.4-fold longer residence time than ^{177}Lu-EB-TATE in the liver (3.28 ± 1.83 *vs.* 0.96 ± 0.16 h, P = 0.21). Regarding other major organs, uptake in the heart, spleen, and kidneys were comparable between the two radiotherapeutic agents. Regarding the effective half-life and residence time, both radioligands

Table 2 Maximum grade of hematotoxicity possibly, probably, or definitely related to treatment.

Patient	Hb toxicity			WBC toxicity			ANC toxicity			PLT toxicity			Total RMD (Gy)	T1-T2 gap (weeks)
	Before therapy	After first PRRT	After second PRRT	Before therapy	After first PRRT	After second PRRT	Before therapy	After first PRRT	After second PRRT	Before therapy	After first PRRT	After second PRRT		
Group A														
LNC1010-1	0	0	0	0	0	0	0	0	0	0	0	0	0.99	8
LNC1010-2	0	0	0	0	0	0	0	0	2	0	0	0	0.78	8
LNC1010-3	0	0	0	0	2	2	0	1	1	0	1	2	0.75	8
Group B														
LNC1010-4	0	0	2	0	1	**3**	0	1	2	0	0	**4**	**1.51**	8
LNC1010-5	0	0	0	0	0	1	0	0	0	0	0	2	0.64	8
LNC1010-6	0	0	0	0	0	0	0	0	0	0	0	1	0.92	8
LNC1010-7a	0	2	2	0	0	0	0	0	0	0	0	2	0.93	8
LNC1010-8a	2	2	2	0	2	2	0	2	2	0	2	2	1.08	10
LNC1010-9a	0	0	1	0	2	1	0	2	0	0	2	1	0.77	8
Group C														
LNC1010-10	2	2	**4**	0	1	**3**	0	1	**4**	0	0	**4**	**2.41**	8
LNC1010-11	0	0	0	0	0	0	0	0	0	0	0	0	1.58	8
LNC1010-12	2	**3**	**3**	0	2	0	0	1	0	0	**3**	**4**	**1.96**	11
Group D														
EB-TATE-1	2	1	1	0	0	1	0	0	0	0	0	1	1.07	8
EB-TATE-2	0	0	0	0	2	0	0	2	0	0	1	0	0.89	8
EB-TATE-3	0	2	2	0	2	2	0	2	**3**	0	**3**	**3**	1.05	10

PLT: platelets; Hb: hemoglobin; WBC: white blood cell; ANC: absolute neutrophil count; RMD: red marrow dose.

Total RMD is the total radiation absorbed dose of red bone marrow administered for all ^{177}Lu-LNC1010, based on dosimetric dose estimates of red bone marrow. aDue to the occurrence of Grade 4 hematological toxicity in Patient LNC1010-4, three additional patients (Patients LNC1010-7, 8, and 9) were enrolled at the same dose level.

T1-T2 gap is normally 8 weeks, but the timing of the second treatment is adjusted appropriately according to the maximum grade of hematologic toxicity after the first treatment.

All related hematologic toxicities of grade 3 or above occurring during the PRRT treatment are displayed in bold.

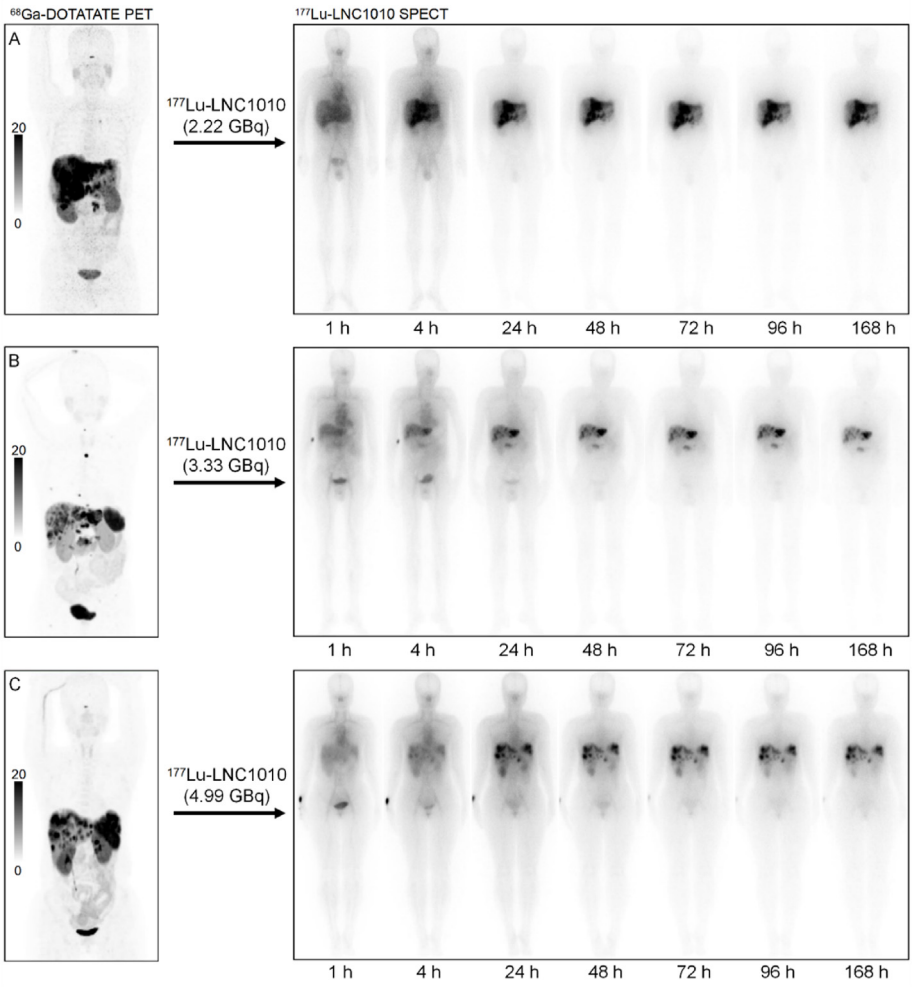

Figure 4 Three patients with metastatic NETs received PRRT with different doses of ^{177}Lu-LNC1010 (A: 2.22 GBq; B: 3.33 GBq; C: 4.99 GBq).^{68}Ga-DOTATATE PET/CT scans (left) were performed for screening before ^{177}Lu-LNC1010-based PRRT, revealing intense radioactive uptake in metastatic lesions. On post-therapeutic WBS (anterior views) from 1 to 168 h post injection in the three patients (right), ^{177}Lu-LNC1010 exhibited relatively high uptake in the bloodstream at 1 h post injection and significant ^{177}Lu-LNC1010 uptake and retention in metastatic lesions at 24−168 h post injection, which coincided with pre-therapeutic ^{68}Ga-DOTATATE PET/CT findings.

exhibited comparable patterns among most major organs, including the heart, kidneys, spleen, and urinary bladder (Fig. 5).

Regarding the tumor dosimetry, the dosimetry for the liver and lymph node metastases was analyzed separately, as the majority of NETs were lymph node and liver metastases. Regarding the time−activity curves, the initial uptake in liver metastases was comparable between ^{177}Lu-LNC1010 and ^{177}Lu-EB-TATE. However, ^{177}Lu-LNC1010 showed a swift initial ascent from the first scan up to 24 h after injection, later decreasing at a slower rate, whereas ^{177}Lu-EB-TATE declined gradually at all time points. In lymph node metastases, the initial ^{177}Lu-LNC1010 uptake was remarkably higher than that of ^{177}Lu-EB-TATE (percentage injected activity: 12% *vs.* 4.5%), followed by a slower ^{177}Lu-LNC1010 decline, demonstrating a 1.4-fold longer effective half-life in all metastatic lesions ($P = 0.04$), a slightly higher effective half-life in liver metastases (144.92 ± 30.90 *vs.* 132.48 ± 9.99 h, $P = 0.73$), and a 1.8-fold longer half-life in lymph node metastases (153.14 ± 50.02 *vs.* 83.78 ± 13.53, $P = 0.07$) than ^{177}Lu-EB-TATE. Similarly, ^{177}Lu-LNC1010 tumor residence time was 2.3-, 2.0-, and 2.5-fold longer in lymph node metastases (0.60 ± 0.18 h *vs.* 0.26 ± 0.07 h, $P = 0.01$), liver metastases (1.20 ± 0.96 h *vs.* 0.59 ± 0.08 h, $P = 0.03$), and all metastatic lesions (0.98 ± 0.81 h *vs.* 0.40 ± 0.19 h, $P < 0.01$) than ^{177}Lu-EB-TATE, respectively. Moreover, ^{177}Lu-LNC1010 exhibited significantly higher absorbed doses in metastatic NETs than in unaffected organs, with 3.0-, 2.7-, and 4.0-fold higher absorbed doses in all tumor lesions (2.14 ± 1.41 Gy/GBq *vs.* 0.71 ± 0.13 Gy/GBq, $P < 0.01$), the lymph node (1.69 ± 0.64 Gy/GBq *vs.* 0.62 ± 0.06 Gy/GBq, $P = 0.01$), and liver metastases (3.33 ± 0.78 Gy/GBq *vs.* 0.84 ± 0.07 Gy/GBq, $P < 0.01$), respectively, than ^{177}Lu-EB-TATE (Fig. 6).

3.10. *Efficacy*

Preliminary anti-tumor efficacy was evaluated 8 weeks after the second PRRT cycle in accordance with RECIST 1.1. Among the 12 patients treated with ^{177}Lu-LNC1010, partial response was seen in 5 (42%), stable disease in another 5 (42%), and progressive disease in 2 patients (17%). Representative cases of tumor responses to ^{177}Lu-LNC1010 are shown in Fig. 7. In addition to

Table 3 Estimated absorbed dose after intravenous administration of ^{177}Lu-LNC1010 and ^{177}Lu-EB-TATE.

Target organ	^{177}Lu-LNC1010		^{177}Lu-EB-TATE	
	Mean (mSv/MBq)	SD (mSv/MBq)	Mean (mSv/MBq)	SD (mSv/MBq)
Adrenals	0.23	0.05	0.23	0.01
Brain	0.18	0.03	0.19	0.02
Breasts	0.20	0.01	0.20	
Esophagus	0.19	0.03	0.20	0.02
Eyes	0.18	0.03	0.19	0.02
Gallbladder wall	0.20	0.03	0.20	0.02
Left colon	0.20	0.03	0.20	0.02
Small intestine	0.19	0.03	0.20	0.02
Stomach wall	0.20	0.03	0.20	0.02
Right colon	0.19	0.03	0.20	0.02
Rectum	0.19	0.03	0.20	0.02
Heart wall	0.58	0.14	0.58	0.02
Kidneys	1.91	0.60	2.47	0.48
Liver	0.25	0.18	0.07	0.00
Lungs	0.19	0.03	0.20	0.02
Ovaries	0.21	0.01	0.21	
Pancreas	0.20	0.03	0.20	0.02
Prostate	0.16	0.02	0.19	0.03
Salivary glands	0.18	0.03	0.19	0.02
Red marrow	0.17	0.04	0.15	0.02
Osteogenic cells	0.20	0.02	0.21	0.03
Spleen	2.53	2.13	2.27	0.04
Testes	0.16	0.02	0.19	0.02
Thymus	0.19	0.03	0.20	0.02
Thyroid	0.19	0.03	0.19	0.03
Urinary bladder wall	0.32	0.08	0.32	0.10
Uterus	0.21	0.01	0.21	
Total body	0.21	0.03	0.21	0.02
Effective dose	0.23	0.06	0.23	0.08

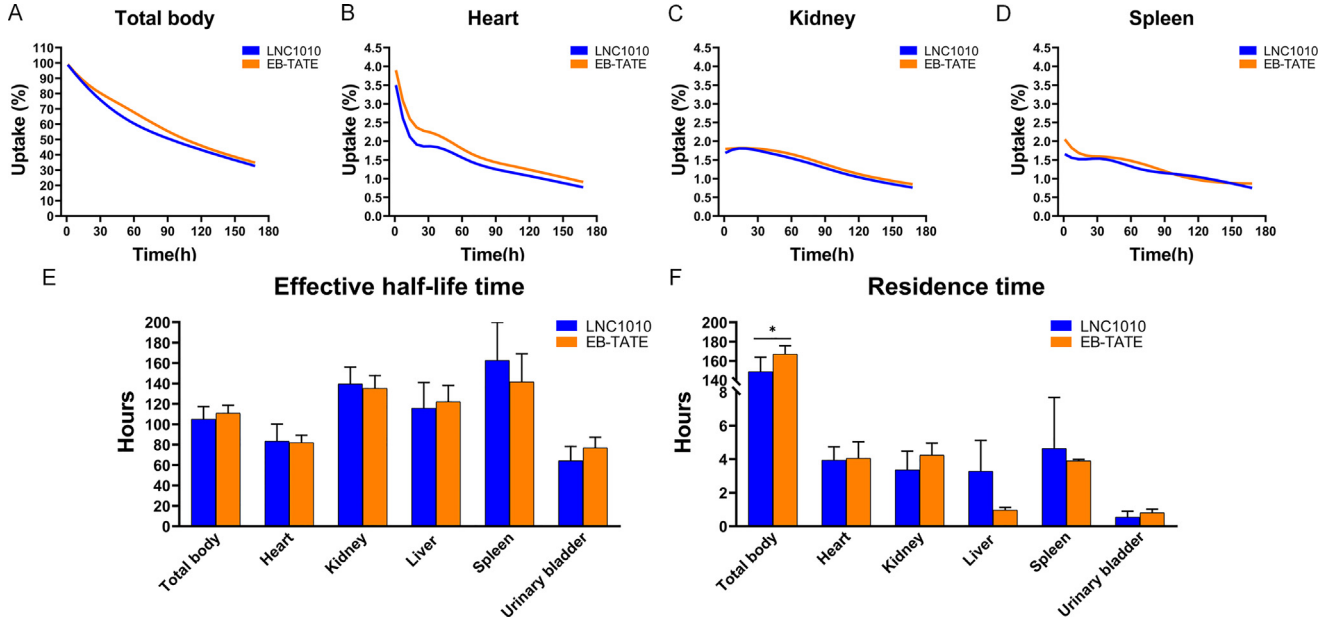

Figure 5 Comparison of biodistribution and dosimetry results for unaffected organs between ^{177}Lu-LNC1010 and ^{177}Lu-EB-TATE: (A–D) uptakes in percentage administered activity in the total body, heart, kidney, liver, and spleen (%); (E) effective half-life (h); and (F) residence time (h). Data present as mean ± SD. The asterisk (*) indicates a *P*-value less than 0.05.

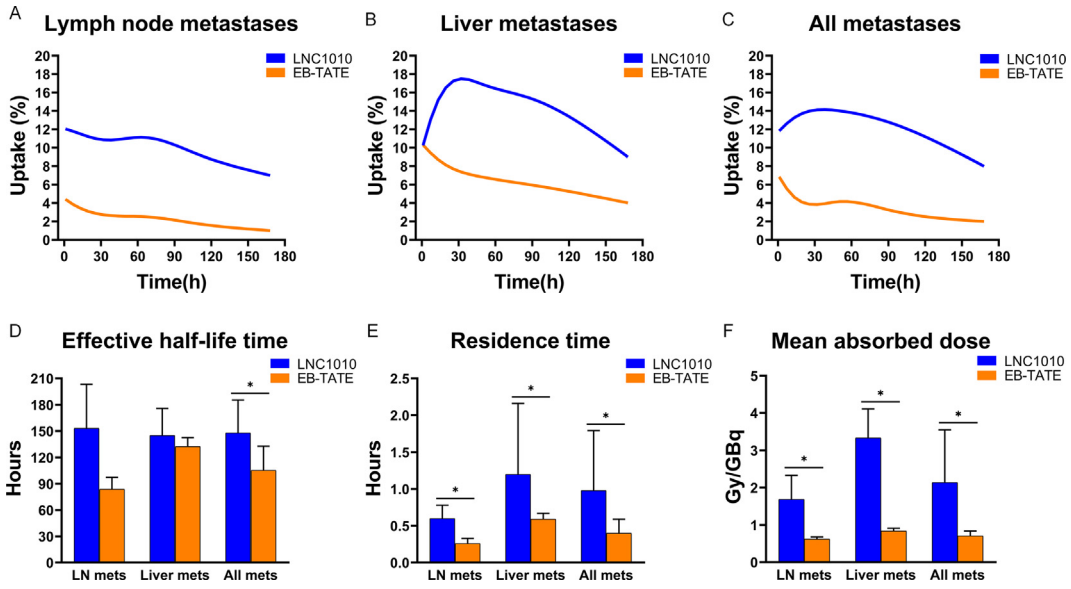

Figure 6 Comparison of biodistribution and dosimetry results for metastases between ^{177}Lu-LNC1010 and ^{177}Lu-EB-TATE: (A–C) kinetics of lymph nodes, liver, and all metastases; (D) effective half-life; (E) residence time of metastases (h); and (F) absorbed dose of metastases. Data present as mean ± SD. The asterisk (*) indicates a *P*-value less than 0.05. LN: lymph node; mets: metastases.

tumor size reduction and remission, one patient (Patient 11) experienced symptomatic relief from hypoglycemia after ^{177}Lu-LNC1010 treatment. The ORR and DCR in patients with different NET types were 42% (5/12) and 83% (10/12), respectively (Fig. 8).

4. Discussion

In this study, we designed and comprehensively assessed the biological activity of a second-generation long-acting EB-modified SSA. We designed and developed, ^{177}Lu-LNC1010, in SSTR2-expressing AR42J tumor cells and xenografts to determine its safety, pharmacokinetics, dosimetry, and preliminary efficacy in NETs. Thereafter, we conducted an open-label, non-randomized, first-in-human, dose escalation study of ^{177}Lu-LNC1010 in patients with metastatic/advanced NETs, which demonstrated a good safety profile with tolerable side effects, compared with ^{177}Lu-EB-TATE based PRRT. Moreover, two ^{177}Lu-LNC1010-based PRRT cycles resulted in a 42% ORR and 83% DCR in patients with different NET types, potentially due to

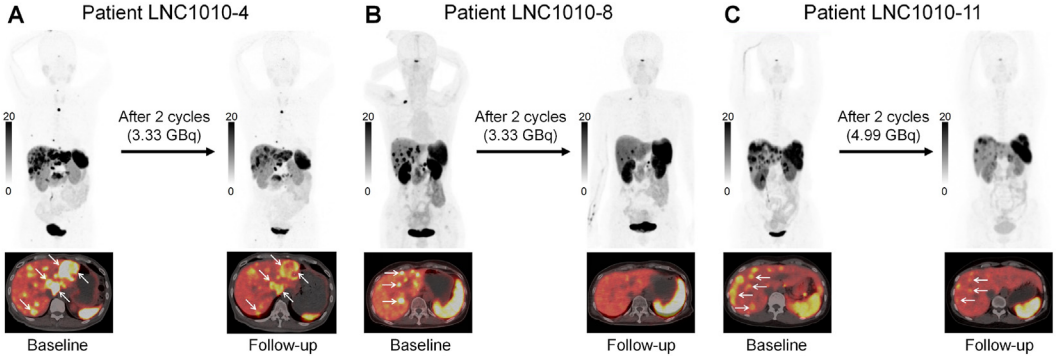

Figure 7 Three patients who responded and achieved a partial disease response after two ^{177}Lu-LNC1010 treatment cycles. (A) A 65-year-old male with metastatic pancreatic NET and disease progression after SSA therapy. Baseline ^{68}Ga-DOTATATE PET/CT revealed intense uptake in primary and metastatic lesions, including the pancreas, liver, lymph node, and bone. After two treatment cycles using 3.33 GBq of ^{177}Lu-LNC1010, follow-up ^{68}Ga-DOTATATE PET/CT showed that the patient responded well to ^{177}Lu-LNC1010-based PRRT and achieved a partial response to the disease. (B) A 55-year-old female with metastatic pancreatic NET and disease progression after surgery and SSA therapy. Baseline ^{68}Ga-DOTATATE PET/CT revealed intense uptake in metastatic lesions, including the pancreas, liver, lymph node, and bone. After two treatment cycles using 3.33 GBq of ^{177}Lu-LNC1010, follow-up ^{68}Ga-DOTATATE PET/CT showed that the patient responded well to ^{177}Lu-LNC1010 -based PRRT and achieved a partial response to the disease. Furthermore, symptoms of abdominal pain and vomiting improved. (C) A 37-year-old female with metastatic pancreatic NET and disease progression after SSA therapy. Baseline ^{68}Ga-DOTATATE PET/CT revealed intense uptake in primary and metastatic lesions, including the pancreas, liver, and spleen. After two treatment cycles using 4.99 GBq of ^{177}Lu-LNC1010, follow-up ^{68}Ga-DOTATATE PET/CT showed that the patient responded well to ^{177}Lu-LNC1010-based PRRT and achieved a partial response to the disease. Furthermore, hypoglycemic symptoms resolved. SSA, somatostatin analog.

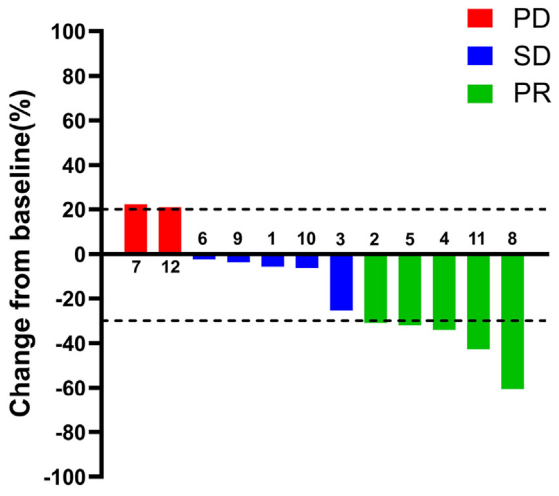

Figure 8 Change from baseline in the sum of the largest diameter of target lesions (n = 12). The patient ID for the LNC1010 group is noted above each response. PD: progressive disease; SD: stable disease; PR: partial response.

high tumor uptake and gradual clearance, leading to an increased tumor radiation dose.

^{177}Lu-EB-TATE (first generation) was previously designed, synthesized, and evaluated in patients with well-differentiated metastatic NETs [6,8,16]. The absorbed dose by the tumor from ^{177}Lu-EB-TATE was notably greater than that from ^{177}Lu-DOTATATE. Interestingly, PRRT with ^{177}Lu-EB-TATE at 0.66 GBq/cycle demonstrated similar therapeutic efficacy to the ^{177}Lu-DOTA-TATE-treated group, as evidenced by the SUV reduction[20]. However, increasing the ^{177}Lu-EB-TATE dose from 1.85 to 3.7 GBq/cycle did not improve ORR and DCR in patients with metastatic NETs[16]. After multiple treatment cycles, patients in the high-dose group (3.7 GBq/cycle) tended to have reduced DCR than those in the median-dose group (1.8 GBq/cycle)[9]. This suggests that excessive radiopharmaceutical doses may not be effectively absorbed by the tumor lesions and instead may be retained in the blood circulation and accumulate in unaffected organs. Therefore, further optimization of the pharmacokinetic and pharmacodynamic characteristics is crucial to ensure therapeutic efficacy while minimizing side effects.

Preclinical evaluation of LNC1010 demonstrated specific and comparable SSTR2-binding affinity to DOTATATE. ^{68}Ga-LNC1010 exhibited high stability *in vivo* and high tumor-to-normal tissue ratios in HPLC and PET image analysis, respectively. SPECT imaging and biodistribution analysis demonstrated that rapid ^{177}Lu-LNC1010 accumulation in tumor lesions resulted in longer tumor retention times than that of ^{177}Lu-DOTATATE. As effective tumor elimination requires a threshold radioactivity concentration to trigger cancer cell death and shrinkage, the increased tumor uptake and improved *in vivo* stability indicate that ^{177}Lu-LNC1010 may be an optimal choice for the treatment NETs.

These preclinical findings supported first-in-human, dose escalation using ^{177}Lu-LNC1010 in patients with metastatic NETs. As expected, ^{177}Lu-LNC1010 exhibited prolonged blood circulation and a slightly shorter biological half-life than that of ^{177}Lu-EB-TATE in all patients. We observed a whole-body absorbed dose to ^{177}Lu-LNC1010 of 0.23 ± 0.06 mSv/MBq, which was higher than that of other studies[21]. The spleen had the highest absorbed dose (2.53 ± 2.13 mSv/MBq), consistent with other study findings[21,22]. Although the kidneys are one of the primary dose-limiting organs in PRRT[23], no short-term nephrotoxicity of any grade was reported in this study. According to the widely recognized upper limit of the absorbed dose to the kidneys, which is between 23 and 29 Gy (Gy)[24–26], an accumulated dose of 12–15 GBq ^{177}Lu-LNC1010 was administered to patients. Dosimetry results suggested that up to four ^{177}Lu-LNC1010 PRRT cycles (3.33 Gq/cycle) may be feasible. In previous studies, the long-term severe grade (G3/G4) nephrotoxicity was minimal; no statistically significant difference regarding the creatinine levels was observed between the standard (PRRT = 4 cycles) and extended treatment groups (PRRT >4 cycles) (89.30 ± 51.19 *vs.* 93.20 ± 55.98 μmol/L; P = 0.364), and adverse renal events exhibited only a marginal increase rising from 0.4% of patients in the standard group to 1.1% in the extended treatment group[27,28]. In addition, this limited dose of 23 Gy to the kidneys which was previously extrapolated from external-beam radiation therapy (EBRT) may not be directly translatable to PRRT, particularly with the long-acting somatostatin analog ^{177}Lu-LNC1010 since it is characterized by a sustained but lower radiation dose rate, and the different physical properties of the radioactive particles[29]. Therefore, the maximal administration of ^{177}Lu-LNC1010 based on kidney tolerance might be more than 4 cycles, and careful dose administration is required when considering multiple PRRT cycles.

^{177}Lu-LNC1010 exhibited a slightly higher radiation dose in the liver than ^{177}Lu-EB-TATE. While PRRT-related hepatotoxicity is typically mild and rare[30], one patient experienced G3 hepatotoxicity and another experienced G4 hepatotoxicity in this study after the first ^{177}Lu-LNC1010 and ^{177}Lu-EB-TATE treatment cycle, respectively. However, both patients had NETs with diffuse liver metastases, which typically increases the liver burden significantly, serving as a major factor influencing hepatotoxicity[31].

Subacute G3–G4 blood-related toxicity was seen in 25% of patients administered ^{177}Lu-LNC1010, primarily in those receiving a high therapeutic dose (4.99 GBq/cycle). PRRT often induces hematologic toxicity due to radiation exposure to the bone marrow. In our study, exposure of ^{177}Lu-LNC1010 to the red marrow reached 0.17 ± 0.04 mSv/MBq, which was comparable to ^{177}Lu-EB-TATE (0.15 ± 0.02 mSv/MBq). A positive correlation between hematological toxicity and total RMD was revealed, with patients in the ^{177}Lu-LNC1010 group receiving >1.5 Gy total RMD experiencing G3/G4 thrombocytopenia, while no G3/G4 thrombocytopenia occurred in patients receiving <1.2 Gy total RMD. This suggests a maximum tolerated ^{177}Lu-LNC1010 dose of 3.33 GBq/cycle, with potentially risks outweighing the benefits at higher doses. Previous reports have indicated that somatostatin functions as a chemoattractant based on SSTR-specific expression on immature ($CD34^+$ cells) human and murine hematopoietic precursors[32]. Flow cytometric analysis revealed SSTR expression primarily in $CD34^+$ cells, with the highest expression levels observed in the $CD34^+/CD117^+$ subset[32]. These cells, constituting merely a minor percentage of the bone marrow, cannot be detected using ^{177}Lu-LNC1010 planar WBS. This may explain the G3/G4 hematotoxicity observed when the total RMD did not exceed the widely accepted bone marrow radiation dose limit (2 Gy)[33]. Similarly, a previous phase I study using ^{177}Lu-satoreotide tetraxetan, an SSTR2 antagonist, observed G4 hematologic toxicity in four of seven (57%) patients after two PRRT cycles,

despite a low absorbed dose (0.09 mSv/MBq) in the bone marrow[34].

The positive treatment response to ^{177}Lu-LNC1010 may be attributed to the high radiation doses delivered to metastatic lesions. Although comparable biodistribution and dosimetry results between ^{177}Lu-LNC1010 and ^{177}Lu-EB-TATE were observed in most unaffected organs, ^{177}Lu-LNC1010 exhibited higher uptake, prolonged effective half-life, and residence time than that of ^{177}Lu-EB-TATE in most tumor lesions, resulting in 2.7-, 4.0-, and 3.0-fold higher radiation doses in the metastatic lymph nodes, liver, and other metastases than those of ^{177}Lu-EB-TATE, respectively. However, as two patient cohorts were used to compare the tumor absorbed dose between ^{177}Lu-LNC1010 and ^{177}Lu-EB-TATE, cohort heterogeneity and variations in receptor densities and tumor burdens, led to significant variation in the average tumor-absorbed doses across different patients[18,21]. Therefore, the mean tumor absorbed dose in this study may not be characteristic of different patients or distinct therapy cycles within the same patient. Similarly, direct comparisons of ^{177}Lu-LNC1010 with other PRRT radiopharmaceuticals may not be feasible. Unlike in PET imaging studies, a head-to-head comparison between two therapeutic radiopharmaceuticals in one patient is not possible since the influence of the previous PRRT must be considered[35,36].

Although therapeutic efficacy was not the main emphasis of the current study, preliminary PRRT efficacy results showed an 83% DCR and a 42% ORR after two ^{177}Lu-LNC1010 treatment cycles. Even then the DCR appear to be commensurate with those previously reported for ^{177}Lu-satoreotide tetraxetan (85% DCR) and ^{177}Lu-LM3 (85.1% DCR), it should be noted that our patient cohort received only two cycles of PRRT, which is less than the therapeutic cycles in the PRRT study with ^{177}Lu-LM3 (up to four cycles). Furthermore, our research protocol was designed as a dose-escalation study; therefore, a subgroup of patients was treated with lower therapeutic doses (*e.g.*, 60−100 mCi) than the doses in regular PRRT studies (200 mCi)[34,37]. Therefore, the therapeutic efficacy of ^{177}Lu-LNC1010 will be further evaluated in future phase II and phase III clinical trials and compared with FDA-approved Lutathera (^{177}Lu-DOTATATE).

This study has a few limitations. First, the small patient population and limited number of patients who received ^{177}Lu-EB-TATE treatment for comparison warrants further randomized, controlled studies with larger sample sizes. Second, this study does not directly compare the effectiveness and safety of ^{177}Lu-LNC1010 *versus* ^{177}Lu-EB-TATE, but instead relies on observations from separate patient cohorts, with 12 individuals receiving ^{177}Lu-LNC1010 and three controls receiving ^{177}Lu-EB-TATE. Third, this study lacked long-term observations of AEs, including hematologic toxicities and nephrotoxicity; however, these issues will be addressed in subsequent studies.

In conclusion, ^{177}Lu-LNC1010 demonstrated good *in vitro* and *in vivo* stability and SSTR2 binding affinity. Preclinical studies indicated increased absorption and extended retention of ^{177}Lu-LNC1010 in SSTR2 expressing AR42J tumor xenografts. The first-in-human trial revealed higher tumor uptake and absorbed doses with ^{177}Lu-LNC1010 than those with ^{177}Lu-EB-TATE, leading to 83% DCR and 42% ORR after two treatment cycles. In addition, the dose-escalation study identified 3.3 GBq/cycle was the most suitable therapeutic dose for forthcoming trials. While the preliminary data on safety and PRRT efficacy are encouraging, further investigations through multicenter, prospective, and randomized controlled trials are needed.

Acknowledgments

This work was supported by the National Natural Science Foundation of China (No. 82071961), Fujian Research and Training Grants for Young and Middle-aged Leaders in Healthcare, Key Scientific Research Program for Yong Scholars in Fujian (No. 2021ZQNZD016, China), Fujian Natural Science Foundation for Distinguished Young Scholars (No. 2022D005, China), Innovation of Science and Technology, Fujian Province (No. 2021Y9134, China), National University of Singapore (No. NUHSRO/2020/133/Startup/08, NUHSRO/2023/008/NUSMed/TCE/LOA, NUHSRO/2021/034/TRP/09/Nanomedicine), National Medical Research Council (No. MOH-001388-00, MOH-001041, CG21APR1005, Singapore), Singapore Ministry of Education (No. MOE-000387-00, Singapore), and National Research Foundation (No. NRF-000352-00, Singapore).

Author contributions

Wei Guo: Conceptualization, Data curation, Formal analysis, Investigation, Methodology, Writing − original draft, Writing − review & editing. Xuejun Wen: Conceptualization, Formal analysis, Investigation, Methodology, Software, Writing − original draft. Yuhang Chen: Data curation, Investigation, Methodology, Resources, Software, Writing − original draft. Tianzhi Zhao: Data curation, Formal analysis, Software, Visualization. Jia Liu: Formal analysis, Resources, Software, Validation, Visualization. Yucen Tao: Methodology, Resources, Software, Visualization. Hao Fu: Resources, Supervision, Visualization. Hongjian Wang: Data curation, Validation, Visualization. Weizhi Xu: Software, Visualization. Yizhen Pang: Data curation, Software. Liang Zhao: Software, Validation. Jingxiong Huang: Supervision, Resources. Pengfei Xu: Formal analysis, Methodology. Zhide Guo: Methodology. Weibing Miao: Investigation, Project administration, Resources, Supervision, Writing − review & editing, Funding acquisition. Jingjing Zhang: Formal analysis, Investigation, Methodology, Supervision, Writing − review & editing. Xiaoyuan Chen: Funding acquisition, Investigation, Methodology, Project administration, Supervision, Writing − review & editing. Haojun Chen: Conceptualization, Formal analysis, Funding acquisition, Investigation, Methodology, Supervision, Writing − review & editing.

Conflicts of interest

The authors declare no competing interests.

Appendix A. Supporting information

Supporting information to this article can be found online at https://doi.org/10.1016/j.apsb.2024.05.022.

References

1. Krenning EP, De Jong M, Kooij PP, Breeman WA, Bakker WH, De Herder WW, et al. Radiolabelled somatostatin analogue(s) for peptide receptor scintigraphy and radionuclide therapy. *Ann Oncol* 1999;**10**: S23−30.
2. Appetecchia M, Baldelli R. Somatostatin analogues in the treatment of gastroenteropancreatic neuroendocrine tumours, current aspects and new perspectives. *J Exp Clin Cancer Res* 2010;**29**:19.

3. Strosberg J, El-Haddad G, Wolin E, Hendifar A, Yao J, Chasen B, et al. Phase 3 trial of 177Lu-Dotatate for midgut neuroendocrine tumors. *N Engl J Med* 2017;**376**:125−35.
4. Werner RA, Weich A, Kircher M, Solnes LB, Javadi MS, Higuchi T, et al. The theranostic promise for neuroendocrine tumors in the late 2010s-where do we stand, where do we go?. *Theranostics* 2018;**8**:6088−100.
5. Liu Z, Chen X. Simple bioconjugate chemistry serves great clinical advances: albumin as a versatile platform for diagnosis and precision therapy. *Chem Soc Rev* 2016;**45**:1432−56.
6. Tian R, Jacobson O, Niu G, Kiesewetter DO, Wang Z, Zhu G, et al. Evans blue attachment enhances somatostatin receptor subtype-2 imaging and radiotherapy. *Theranostics* 2018;**8**:735−45.
7. Bandara N, Jacobson O, Mpoy C, Chen X, Rogers BE. Novel structural modification based on Evans blue dye to improve pharmacokinetics of a somastostatin-receptor-based theranostic agent. *Bioconjugate Chem* 2018;**29**:2448−54.
8. Zhang J, Wang H, Jacobson O, Cheng Y, Niu G, Li F, et al. Safety, pharmacokinetics, and dosimetry of a long-acting radiolabeled somatostatin analog ^{177}Lu-DOTA-EB-TATE in patients with advanced metastatic neuroendocrine tumors. *J Nucl Med* 2018;**59**:1699−705.
9. Liu Q, Zang J, Sui H, Ren J, Guo H, Wang H, et al. Peptide receptor radionuclide therapy of late-stage neuroendocrine tumor patients with multiple cycles of ^{177}Lu-DOTA-EB-TATE. *J Nucl Med* 2021;**62**:386−92.
10. Walsh SJ, Bargh JD, Dannheim FM, Hanby AR, Seki H, Counsell AJ, et al. Site-selective modification strategies in antibody−drug conjugates. *Chem Soc Rev* 2021;**50**:1305−53.
11. Huang W, Wu X, Gao X, Yu Y, Lei H, Zhu Z, et al. Maleimide-thiol adducts stabilized through stretching. *Nat Chem* 2019;**11**:310−9.
12. Estrela JM, Ortega A, Obrador E. Glutathione in cancer biology and therapy. *Crit Rev Clin Lab Sci* 2006;**43**:143−81.
13. Wen X, Xu P, Shi M, Liu J, Zeng X, Zhang Y, et al. Evans blue-modified radiolabeled fibroblast activation protein inhibitor as long-acting cancer therapeutics. *Theranostics* 2022;**12**:422−33.
14. Wen X, Xu P, Zeng X, Liu J, Du C, Zeng X, et al. Development of [^{177}Lu]Lu-LNC1003 for radioligand therapy of prostate cancer with a moderate level of PSMA expression. *Eur J Nucl Med Mol Imag* 2023;**50**:2846−60.
15. Fu H, Huang J, Zhao T, Wang H, Chen Y, Xu W, et al. Fibroblast activation protein-targeted radioligand therapy with ^{177}Lu-EB-FAPI for metastatic radioiodine-refractory thyroid cancer: first-in-human, dose-escalation study. *Clin Cancer Res* 2023;**29**:4740−50.
16. Liu Q, Cheng Y, Zang J, Sui H, Wang H, Jacobson O, et al. Dose escalation of an Evans blue-modified radiolabeled somatostatin analog ^{177}Lu-DOTA-EB-TATE in the treatment of metastatic neuroendocrine tumors. *Eur J Nucl Med Mol Imag* 2020;**47**:947−57.
17. Baum RP, Schuchardt C, Singh A, Chantadisai M, Robiller FC, Zhang J, et al. Feasibility, biodistribution, and preliminary dosimetry in peptide-targeted radionuclide therapy of diverse adenocarcinomas using ^{177}Lu-FAP-2286: first-in-humans results. *J Nucl Med* 2022;**63**:415−23.
18. Schuchardt C, Kulkarni HR, Prasad V, Zachert C, Müller D, Baum RP. The Bad Berka dose protocol: comparative results of dosimetry in peptide receptor radionuclide therapy using ^{177}Lu-DOTATATE, ^{177}Lu-DOTANOC, and ^{177}Lu-DOTATOC. *Recent Results Cancer Res* 2013;**194**:519−36.
19. Schuchardt C, Zhang J, Kulkarni HR, Chen X, Müller D, Baum RP. Prostate-specific membrane antigen radioligand therapy using ^{177}Lu-PSMA I&T and ^{177}Lu-PSMA-617 in patients with metastatic castration-resistant prostate cancer: comparison of safety, biodistribution, and dosimetry. *J Nucl Med* 2022;**63**:1199−207.
20. Wang H, Cheng Y, Zhang J, Zang J, Li H, Liu Q, et al. Response to single low-dose ^{177}Lu-DOTA-EB-TATE treatment in patients with advanced neuroendocrine neoplasm: a prospective pilot study. *Theranostics* 2018;**8**:3308−16.
21. Wehrmann C, Senftleben S, Zachert C, Müller D, Baum RP. Results of individual patient dosimetry in peptide receptor radionuclide therapy with ^{177}Lu DOTA-TATE and ^{177}Lu DOTA-NOC. *Cancer Biother Radiopharm* 2007;**22**:406−16.
22. Bodei L, Cremonesi M, Grana CM, Fazio N, Iodice S, Baio SM, et al. Peptide receptor radionuclide therapy with ^{177}Lu-DOTATATE: the IEO phase I-II study. *Eur J Nucl Med Mol Imag* 2011;**38**:2125−35.
23. van Essen M, Krenning EP, Kam BL, De Jong M, Valkema R, Kwekkeboom DJ. Peptide-receptor radionuclide therapy for endocrine tumors. *Nat Rev Endocrinol* 2009;**5**:382−93.
24. Kwekkeboom DJ, de Herder WW, Kam BL, van Eijck CH, van Essen M, Kooij PP, et al. Treatment with the radiolabeled somatostatin analog [^{177}Lu-DOTA 0,Tyr3]octreotate: toxicity, efficacy, and survival. *J Clin Oncol* 2008;**26**:2124−30.
25. Cives M, Strosberg J. Radionuclide therapy for neuroendocrine tumors. *Curr Oncol Rep* 2017;**19**:1−9.
26. Del Prete M, Buteau FA, Beauregard JM. Personalized ^{177}Lu-octreotate peptide receptor radionuclide therapy of neuroendocrine tumours: a simulation study. *Eur J Nucl Med Mol Imag* 2017;**44**:1490−500.
27. Baum RP, Fan X, Jakobsson V, Schuchardt C, Chen X, Yu F, et al. Extended peptide receptor radionuclide therapy: evaluating nephrotoxicity and therapeutic effectiveness in neuroendocrine tumor patients receiving more than four treatment cycles. *Eur J Nucl Med Mol Imag* 2024;**51**:1136−46.
28. Bodei L, Kidd M, Paganelli G, Grana CM, Drozdov I, Cremonesi M, et al. Long-term tolerability of PRRT in 807 patients with neuroendocrine tumours: the value and limitations of clinical factors. *Eur J Nucl Med Mol Imag* 2015;**42**:5−19.
29. Baum RP, Fan X, Jakobsson V, Fei Y, Schuchardt C, Chen X, et al. Long-term nephrotoxicity after PRRT: myth or reality. *Theranostics* 2024;**14**:451−9.
30. Riff BP, Yang YX, Soulen MC, Pryma DA, Bennett B, Wild D, et al. Peptide receptor radionuclide therapy-induced hepatotoxicity in patients with metastatic neuroendocrine tumors. *Clin Nucl Med* 2015;**40**:845−50.
31. Frilling A, Li J, Malamutmann E, Schmid KW, Bockisch A, Broelsch CE. Treatment of liver metastases from neuroendocrine tumours in relation to the extent of hepatic disease. *Br J Surg* 2009;**96**:175−84.
32. Oomen SP, van Hennik PB, Antonissen C, Lichtenauer-Kaligis EG, Hofland LJ, Lamberts SW, et al. Somatostatin is a selective chemoattractant for primitive ($CD34^+$) hematopoietic progenitor cells. *Exp Hematol* 2002;**30**:116−25.
33. Wahl RL, Sgouros G, Iravani A, Jacene H, Pryma D, Saboury B, et al. Normal-tissue tolerance to radiopharmaceutical therapies, the knowns and the unknowns. *J Nucl Med* 2021;**62**:23S−35S.
34. Reidy-Lagunes D, Pandit-Taskar N, O'Donoghue JA, Krebs S, Staton KD, Lyashchenko SK, et al. Phase I trial of well-differentiated neuroendocrine tumors (NETs) with radiolabeled somatostatin antagonist ^{177}Lu-satoreotide tetraxetan. *Clin Cancer Res* 2019;**25**:6939−47.
35. Koral KF, Kaminski MS, Wahl RL. Correlation of tumor radiation-absorbed dose with response is easier to find in previously untreated patients. *J Nucl Med* 2003;**44**:1541−3.
36. Sgouros G, Squeri S, Ballangrud ÅM, Kolbert KS, Teitcher JB, Panageas KS, et al. Patient-specific, 3-dimensional dosimetry in non-Hodgkin's lymphoma patients treated with ^{131}I-anti-B1 antibody: assessment of tumor dose-response. *J Nucl Med* 2003;**44**:260−8.
37. Baum RP, Zhang J, Schuchardt C, Müller D, Mäcke H. First-in-humans study of the SSTR antagonist ^{177}Lu-DOTA-LM3 for peptide receptor radionuclide therapy in patients with metastatic neuroendocrine neoplasms: dosimetry, safety, and efficacy. *J Nucl Med* 2021;**62**:1571−81.